GRANT

IN-46-CR

123405

18P

Semi-Annual Reports on

Mesospheric Dynamics and Chemistry from SME Data

by

Darrell F. Strobel

Principal Investigator

Department of Earth and Planetary Sciences

The Johns Hopkins University

Baltimore, MD 21218

July 1, 1986 to December 31, 1987

NAG 5-796

(NASA-CR-182465) MESOSPHERIC DYNAMICS AND CHEMISTRY FROM SME DATA Semiannual Report, 1 Jul. 1986 - 31 Dec. 1987 (Johns Hopkins Univ.) 18 p CSCL 04A

N88-17139

Unclas

G3/46 0123405

The principal research efforts accomplished under NASA grant NAG 5-796 consisted of two parts, which are described in the following two sections.

1. Approximate Algorithm for Computing CO_2 15μ Band Cooling Rates

A fast Curtis matrix calculation of cooling rates due to the 15μ band of CO_2 is modified to parameterize the detailed calculations by Dickinson (1984) of infrared cooling by CO_2 in the mesosphere and lower thermosphere. His calculations included separate NLTE treatment of the different 15μ bands likely to be important for cooling.

Our goal was to compress the detailed properties of the different 15μ bands into a modified Curtis matrix, which represents one composite band with appropriate averaged radiative properties to allow for a simple and quick calculation of cooling rates given a temperature profile.

We use the two-level approach of Houghton (1977) and write the ratio of the collisional deactivation rate of the upper level a_{21}, to its spontaneous decay rate, A_{21}, as

$$\phi = \frac{a_{21}}{A_{21}} = P/0.04mb$$

and introduce the altitude dependent coefficient

$$E_k = (4\pi S n \phi)^{-1}$$

with band strength S and concentration n at discrete heights, k.

The Planck function B(T), the black body emission per unit solid angle per unit area at temperature T, is related to the cooling rate Q, and the total NLTE source function J, by

$$J_k = B_k + E_k Q_k$$

$$Q_k = \sum_j C_{kj} J_j + Q_{SOLAR,k}$$

where C_{kj} is the element of the Curtis matrix and $Q_{SOLAR,k}$ is the solar heating rate (Houghton, 1977). At 15μ solar heating can be ignored. In matrix notation the latter equation may be written

$$Q = CJ \qquad (1)$$

but in the former equation there is no summation and it is incorrect to use matrix multiplication, unless we generalized non-diagonal terms. The source function becomes:

$$J = B + b$$

where

$$(b)_k = E_k Q_k$$

We introduce the matrix Q_{ij} with i the index for height level and j the index for latitude and define

$$(b)_{ij} = \left(E_{ij} Q_{ij}\right)$$

$$J = B + b$$

There is no easy way to invert matrix equation (1). Two methods of solution were tried:

Method 1: The Q dependence of b is assumed to be slowly varying in T, with most temperature information contained in B. Thus b is held constant. This method is only valid when $b^{-1}\partial b/\partial T \ll B^{-1}\partial B/\partial T$.

Method 2: This is an iterative technique in which the temperature profile is used to generate B and the first estimate of Q is given by $Q_o = CB$, $J_1 = B + b_o$, etc. where B is the source function. For the next iteration the source function is $J_1 = B + b_o\ (Q_o)$ and $Q_1 = CJ_1$. This procedure is repeated until convergence is reached.

The following expressions were used

$$B = 97.1(s)\left(\exp\left(\frac{960}{T}\right) - 1\right)^{-1} \qquad E = (4\pi S n \phi)^{-1}$$

$$S = 242\sqrt{\frac{T}{273}}$$

$$J_{ij} = \frac{B_{ij}}{K_2} + K_1(E \cdot Q)_{ij}$$

with additional, adjustable constants K_i introduced to achieve the best accuracy. We selected $K_1 = 4.11 \times 10^{11}$ and $K_2 = 81.12$. These values were chosen because they kept the diagonal Curtis matrix elements near unity.

Inverting the equations to obtain the Curtis matrix C yields an unstable matrix, such that the smallest change in the temperature profile produces large fluctuations in the cooling rates, clearly not desirable.

Our initial trial guess for the Curtis matrix was the identity matrix minus the same constant for all terms, both on and off the diagonal. We assumed that half the radiation would reach space, and chose to absorb 3% of the radiation at each of the 15 levels. As can be seen in Fig. 6, this gave surprisingly close results.

To decrease the error associated with the almost flat matrix, the inverse of the difference between Dickinson's cooling rates and the initial cooling rates was taken. This matrix was also unstable, but it appeared that the columns (involving the coefficients scattering <u>to</u> the same level) were independent, so we constructed a matrix by averaging by the columns. The elements corresponded to ~ 3% absorption at each level and this matrix was added to the previous one. But this resulted in a grossly over corrected cooling profile and consequently only a fraction of the column-like matrix was added to the nearly flat matrix. The resultant matrix yielded cooling rates within a few degrees per day of Dickinson's rates, except in the strongly NLTE region. This final Curtis matrix is given in Table 1. This C matrix generates a better cooling profile than method 1, but is incapable of achieving convergence by method 2.

An alternate approach would be to use a Curtis matrix calculated approximately from first principles and retain K_1 and K_2 as adjustable parameters.

2. Vertical Constituent Transport in the Mesosphere.

Another piece of research, partially supported by this grant, was a study of vertical constituent transport in the mesosphere in collaboration with NRL colleagues (Attachment 1). Ground-based microwave spectroscopy measurements of mesospheric CO and H_2O vertical mixing ratio profiles and SME ozone data were used to infer vertical mixing rates in the upper mesosphere. The CO and H_2O data consistently imply vertical eddy diffusion coefficients in the 70-85 km region of $< (1\text{-}2) \times 10^5$ cm^2 s^{-1} during spring through summer at mid-latitudes. Comparison of SME O_3 data with model results reinforces the conclusion of slow vertical mixing in the upper mesosphere as a consequence of the reduced HO_x catalytic loss of odd oxygen. The slow vertical mixing deduced in this study is consistent with upper limits obtained from studies of the mesospheric heat budget (Apruzese et al., 1984; Strobel et al., 1985) and could be construed as evidence for an advectively controlled mesosphere. A comparison of the vertical eddy diffusion coefficients for momentum stresses, constituent and heat transport suggested that the eddy Prandtl number must of order 10.

References

Apruzese, J. P., D. F. Strobel and M. R. Schoeberl, Parameterization of IR cooling in a middle atmosphere dynamics model. 2. Non-LTE radiative transfer and the globally averaged temperature of the mesosphere and lower thermosphere, J. Geophys. Res., 89, 4917-4926.

Dickinson, R. E., Infrared radiative cooling in the mesosphere and lower thermosphere, J. Atmos. Terr. Phys., 46, 995-1008, 1984.

Houghton, J. H., The Physics of Atmospheres, Cambridge Univ. Press, Cambridge, 203 pp., 1977.

Strobel, D. F., J. P. Apruzese and M. R. Schoeberl, Energy balance constraints on gravity wave induced eddy diffusion in the mesosphere and lower thermosphere, J. Geophys. Res., 90, 13,067-13,072, 1985.

Figure Captions

Fig. 1. Temperature T: the temperature data used by Dickinson, in °K.

Fig. 2. Dickinson cooling calculation Q: the desired complex structure, in °K/day.

Fig. 3. Approximate source function J: in relative units.

Fig. 4. Modified Curtis Approximation QT: cooling calculated by method 1, using the Curtis matrix given in Table 1, in °K/day.

Fig. 5. Error Q-QT: note relatively flat field for all but the upper right positions.

Fig. 6. Initial Curtis Approximation QF, using near flat Curtis matrix, in °K/day.

Fig. 7. Error Q-QF: worse than Q-QT.

Fig. 8. Iterative Approximation Q5: calculated using near flat matrix and only 5 iterations.

Fig. 9. Iterative Approximation QI: calculated using Curtis matrix (Table 1) and 5 iterations.

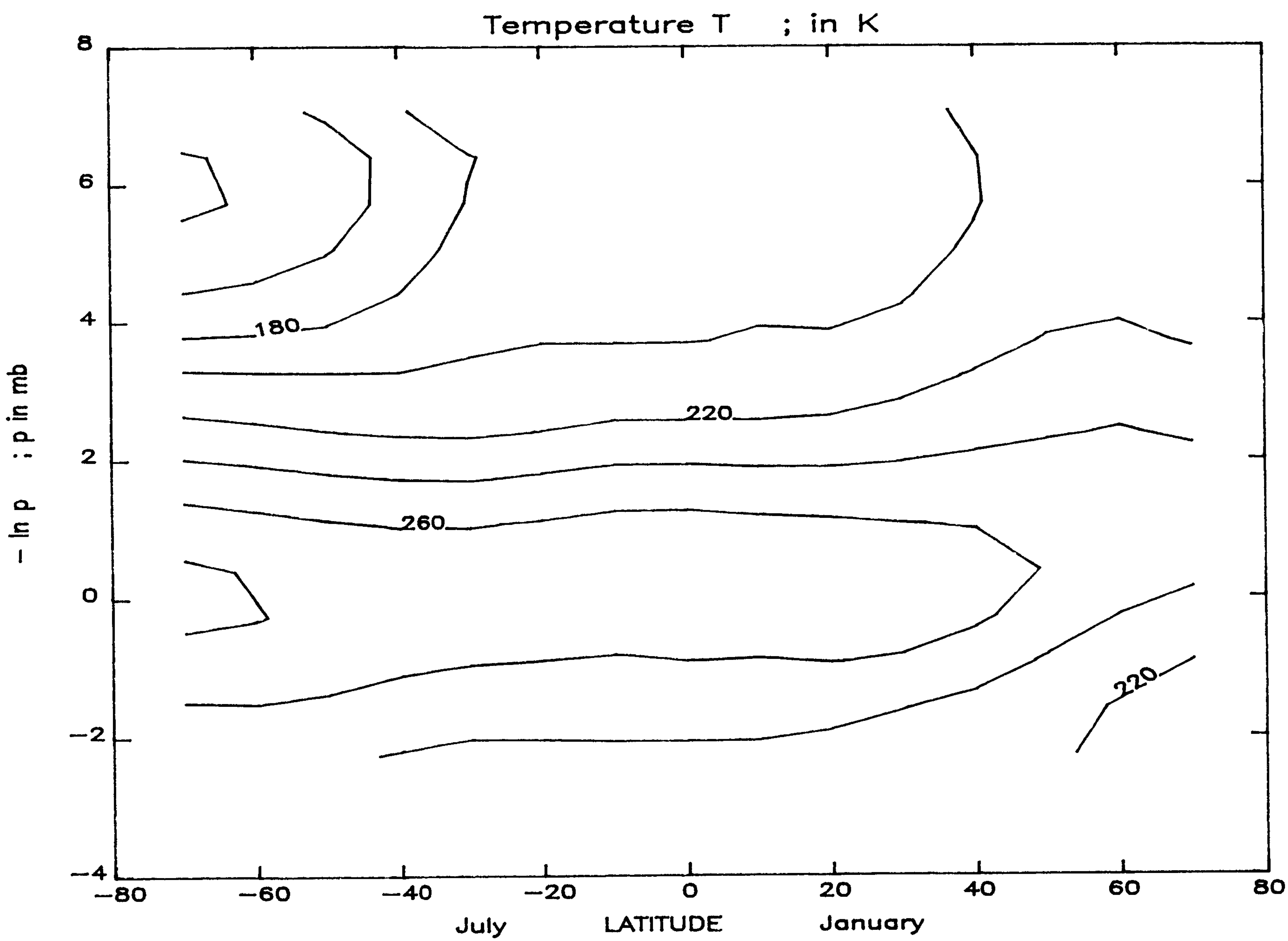
Temperature T ; in K
8
6
4
2
0
−2
−4
− ln p ; p in mb
180
220
260
220
−80
−60
−40
−20
0
20
40
60
80
July
LATITUDE
January

Figure 1

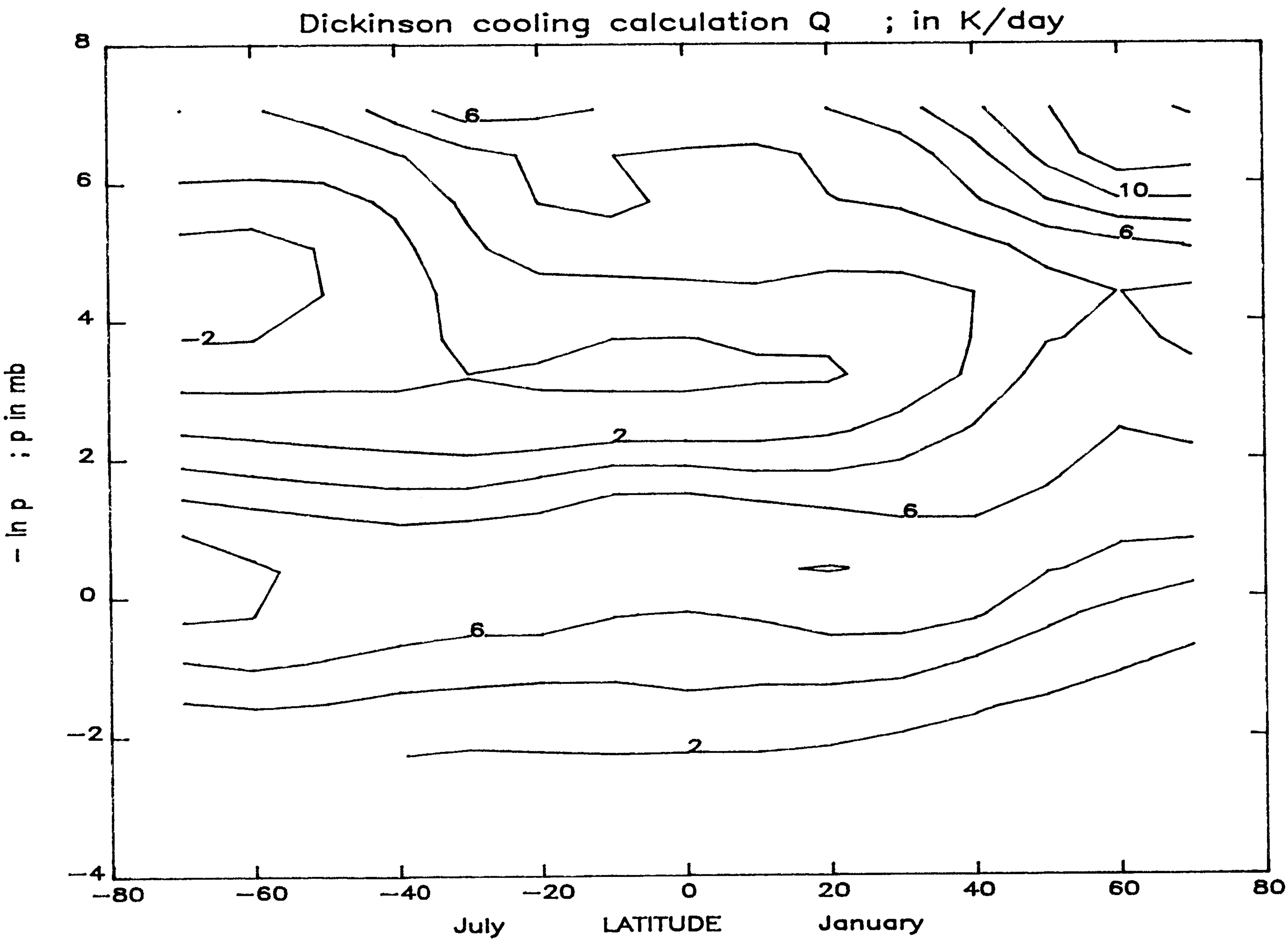
Dickinson cooling calculation Q ; in K/day
- ln p ; p in mb
8
6
4
2
0
−2
−4
−80
−60
−40
−20
0
20
40
60
80
July
LATITUDE
January
10
6
2
−2

Figure 2

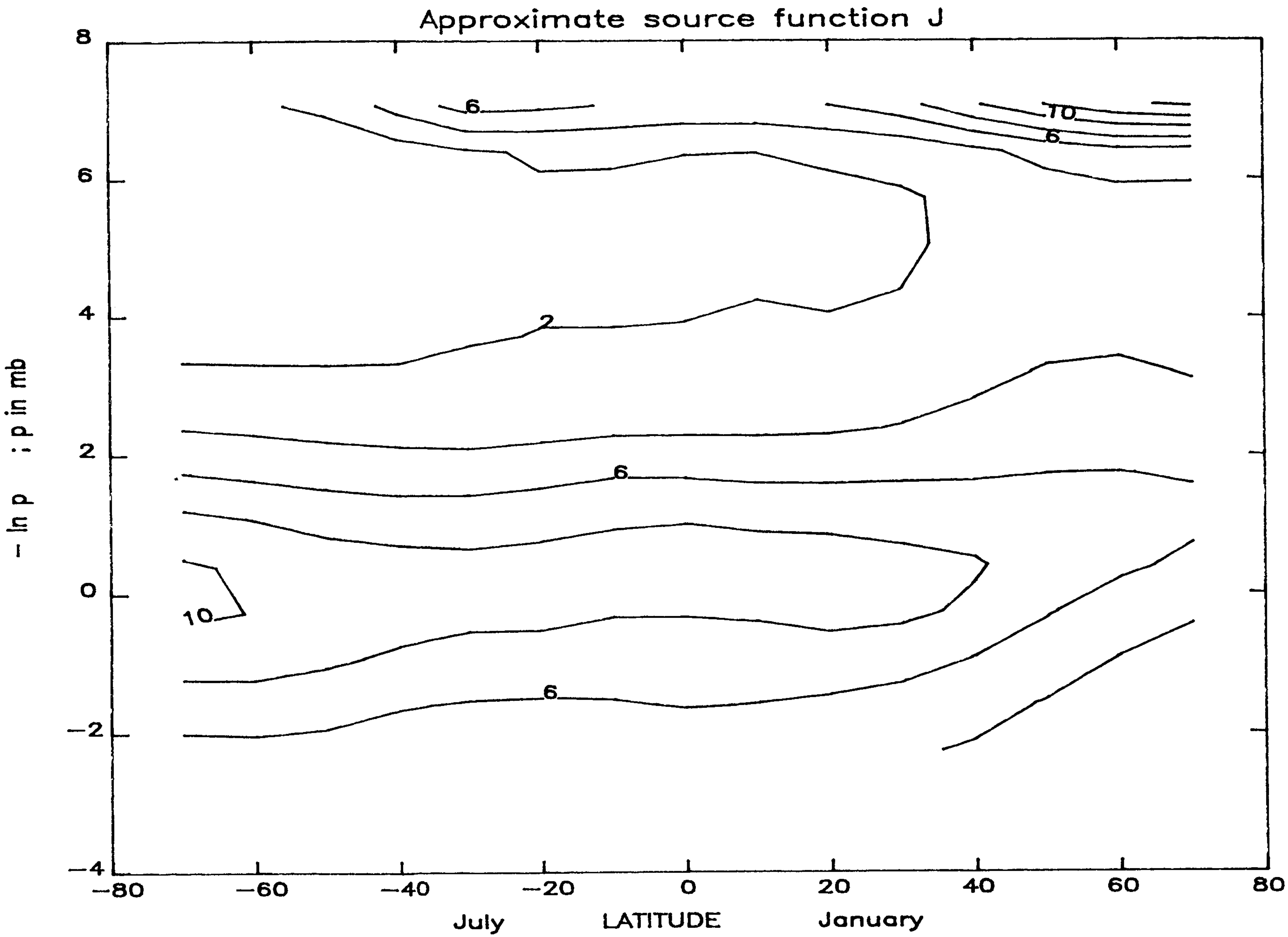
Approximate source function J
8
6
4
2
0
−2
−4
− ln p ; p in mb
−80
−60
−40
−20
0
20
40
60
80
July
LATITUDE
January
6
10
6
2
6
10
6

Figure 3

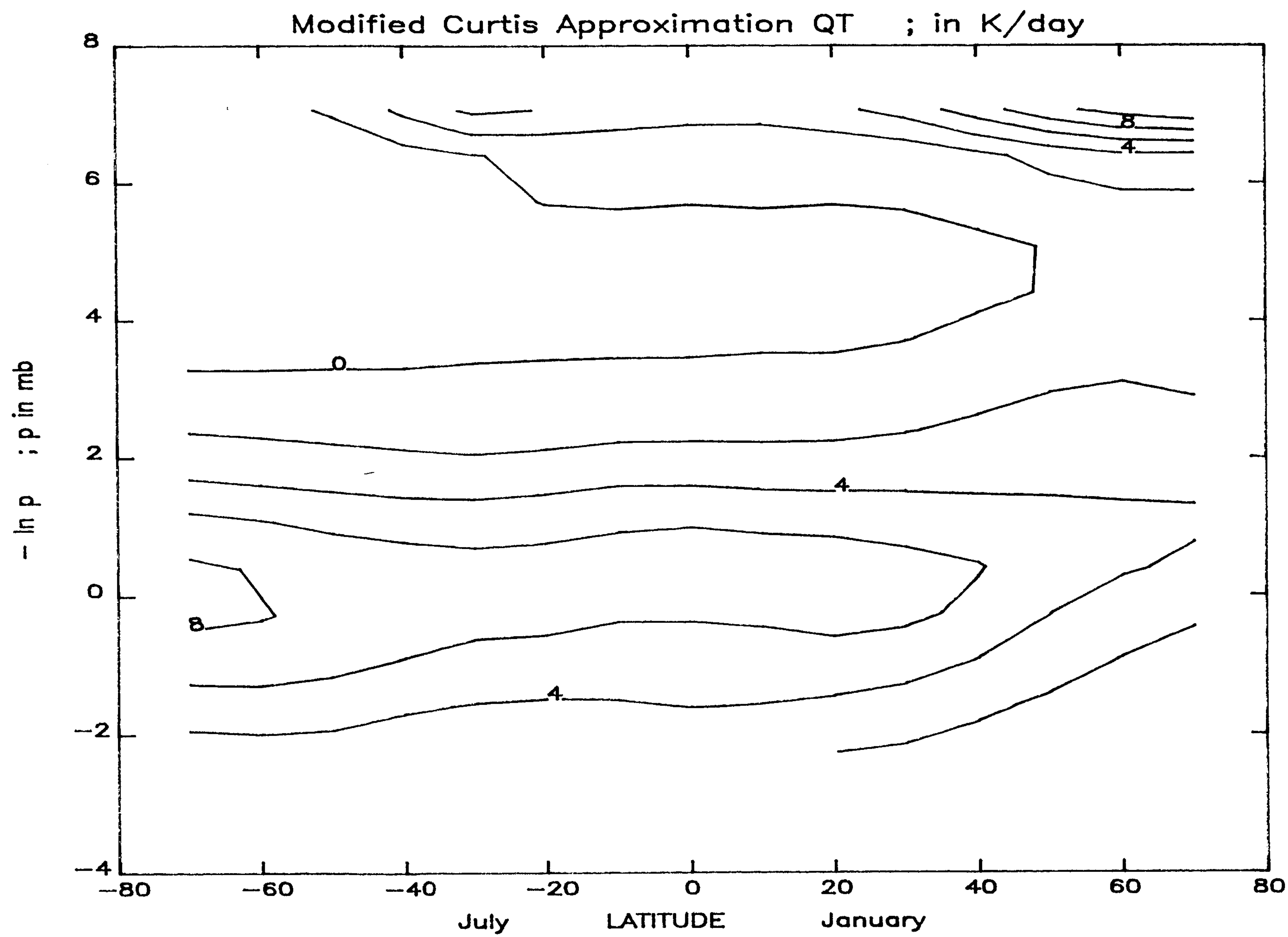
Modified Curtis Approximation QT ; in K/day
− ln p ; p in mb
8
6
4
2
0
−2
−4
−80
−60
−40
−20
0
20
40
60
80
July
LATITUDE
January

Figure 4

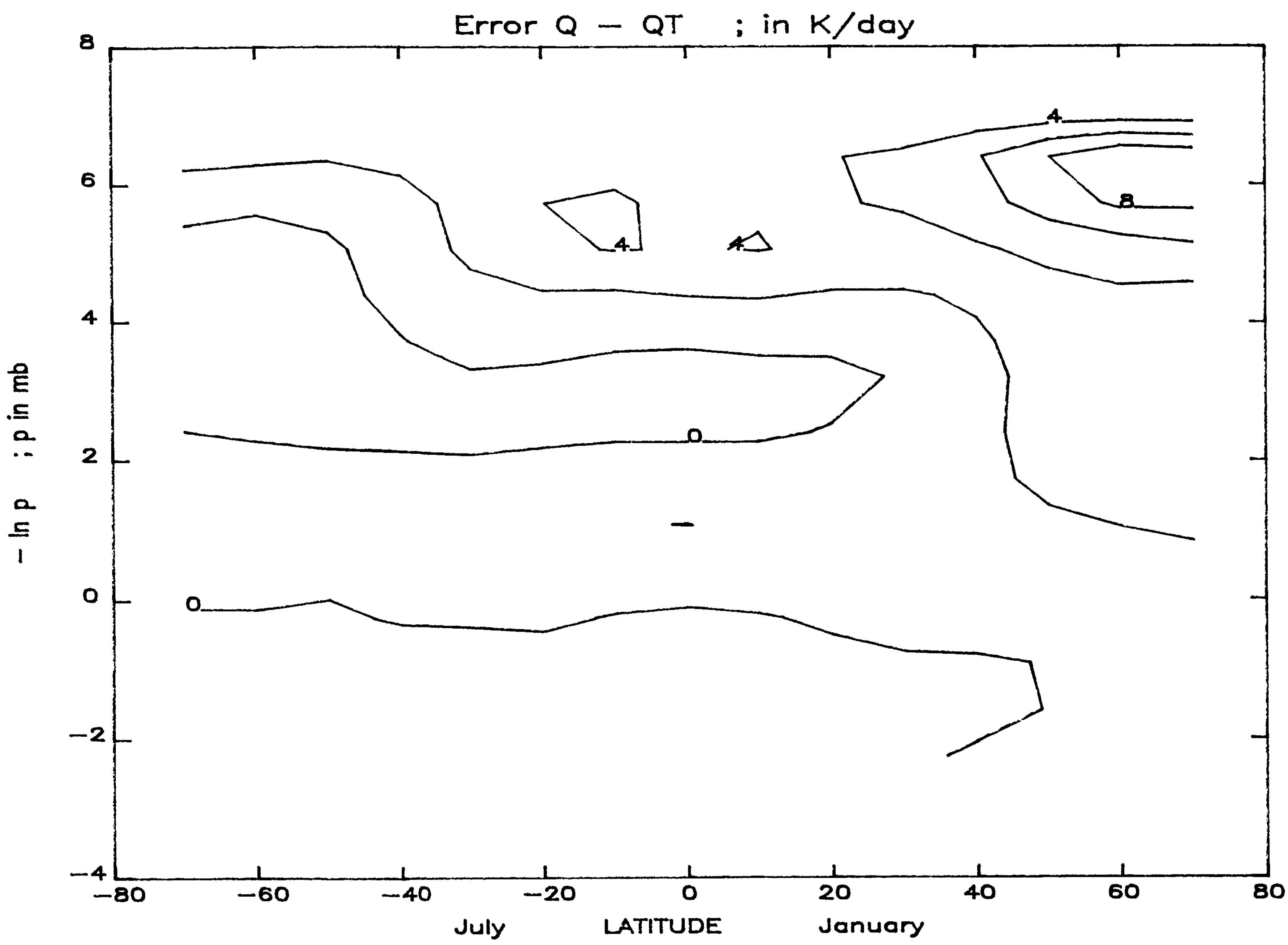
Error Q – QT ; in K/day
8
6
4
2
0
−2
−4
– ln p ; p in mb
4
8
4
4
0
0
−80
−60
−40
−20
0
20
40
60
80
July
LATITUDE
January

Figure 5

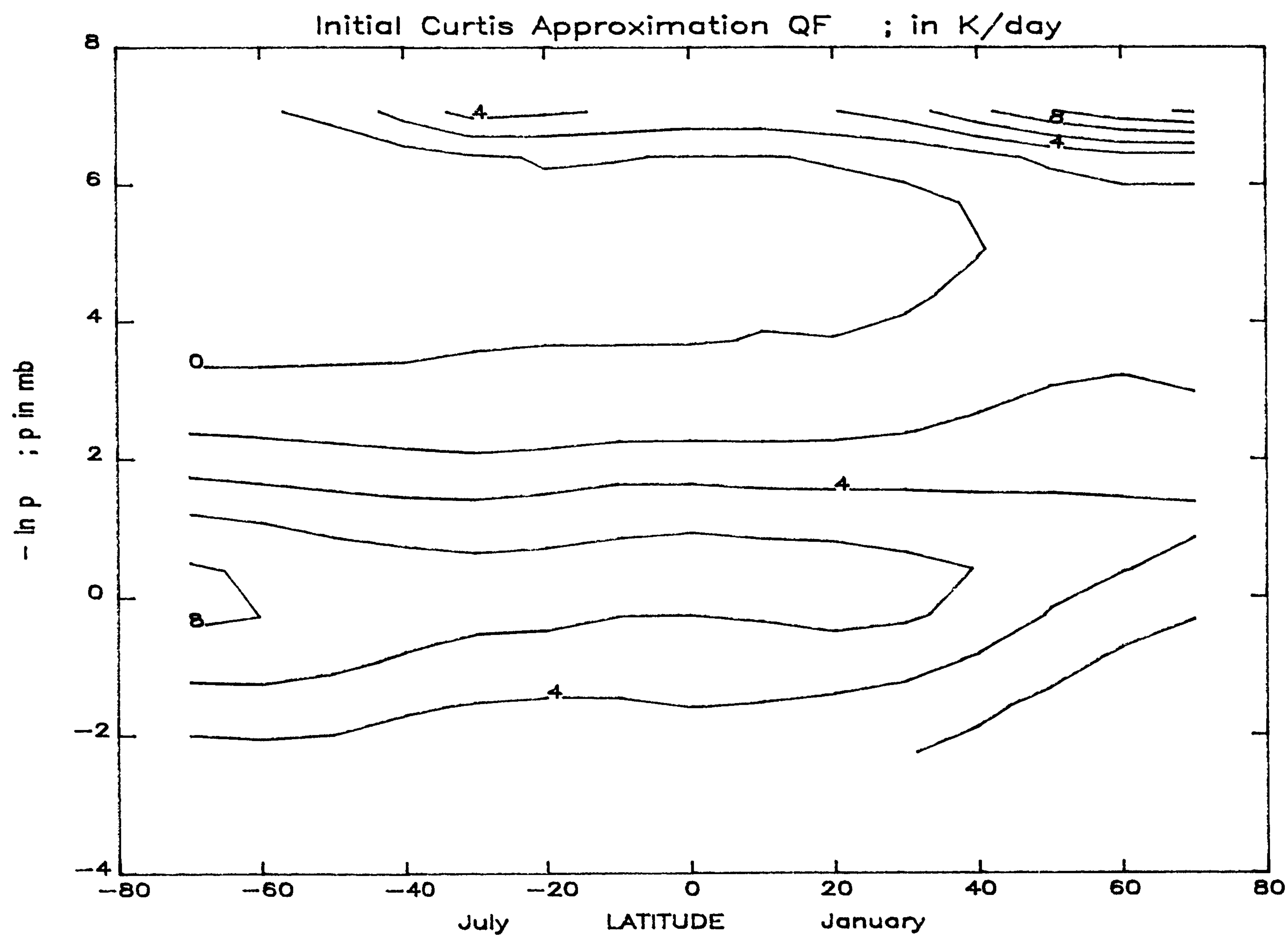

Initial Curtis Approximation QF ; in K/day
8
6
4
2
0
−2
−4
− ln p ; p in mb
−80
−60
−40
−20
0
20
40
60
80
July
LATITUDE
January
4
8
4
0
4
8
4

Figure 6

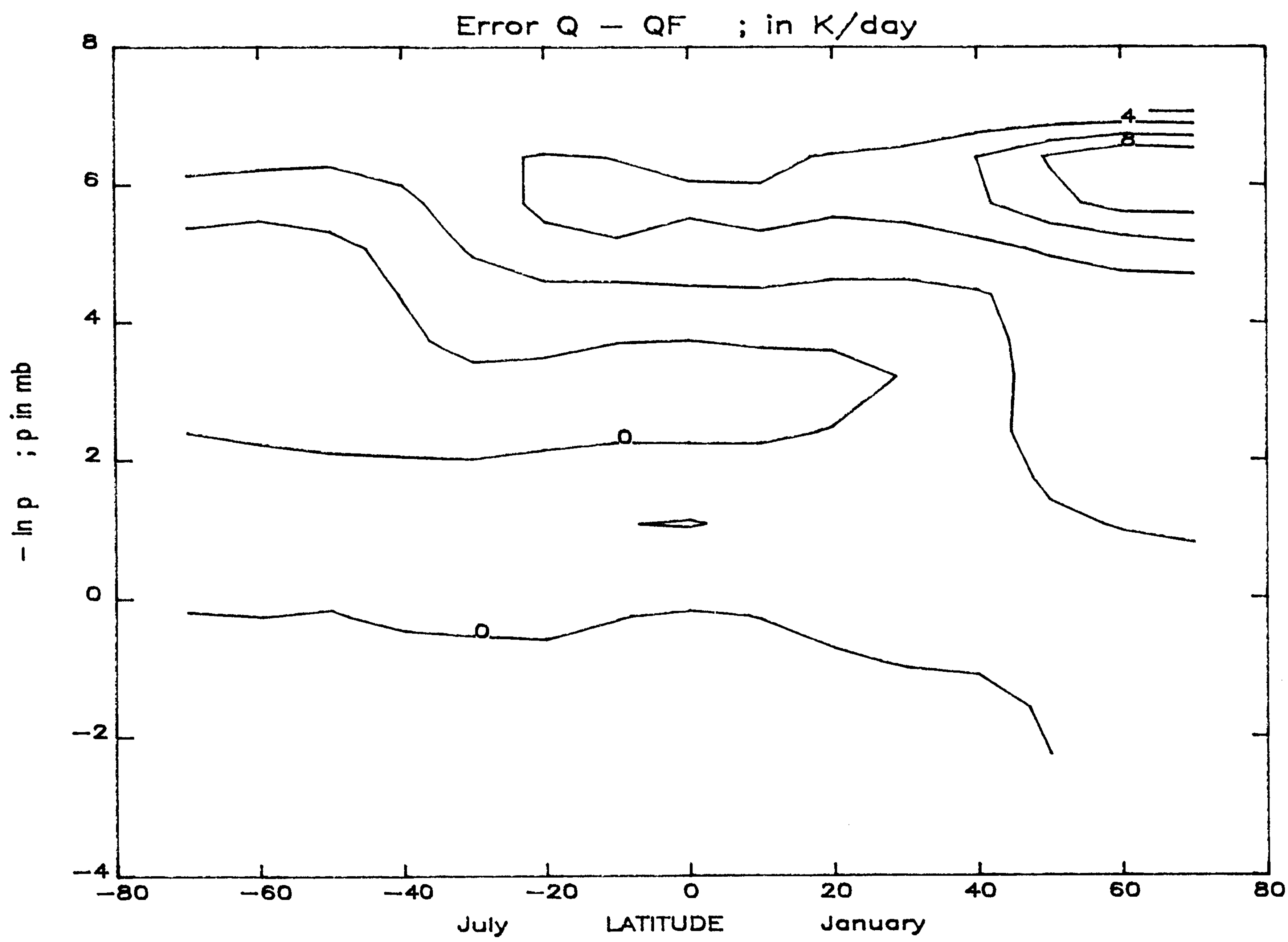

Error Q — QF ; in K/day
8
6
4
2
0
−2
−4
− ln p ; p in mb
−80
−60
−40
−20
0
20
40
60
80
July
LATITUDE
January
0
0
4
8

Figure 7

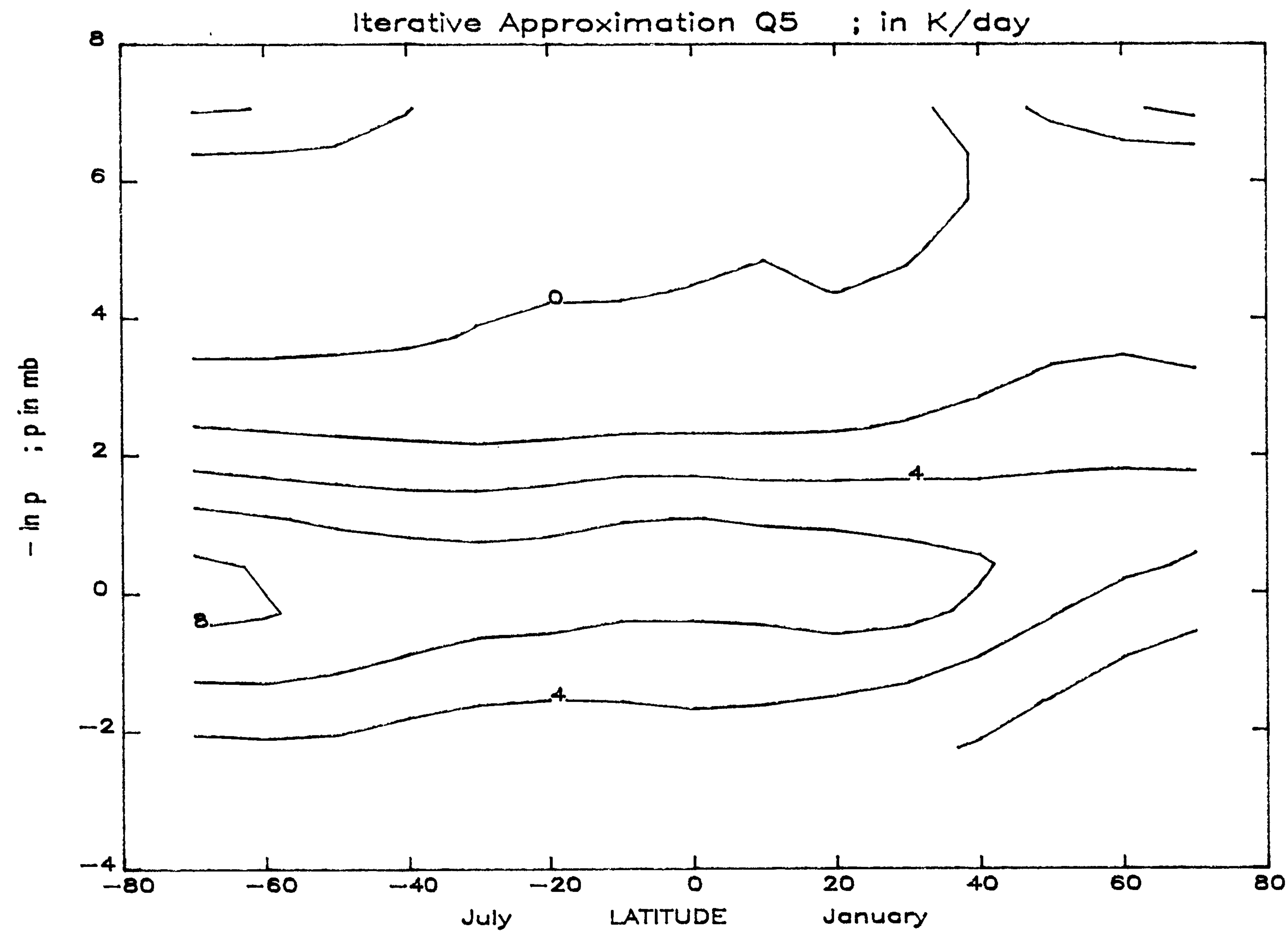
Iterative Approximation Q5 ; in K/day
8
6
4
2
0
−2
−4
− ln p ; p in mb
0
4
8
4
−80
−60
−40
−20
0
20
40
60
80
July
LATITUDE
January

Figure 8

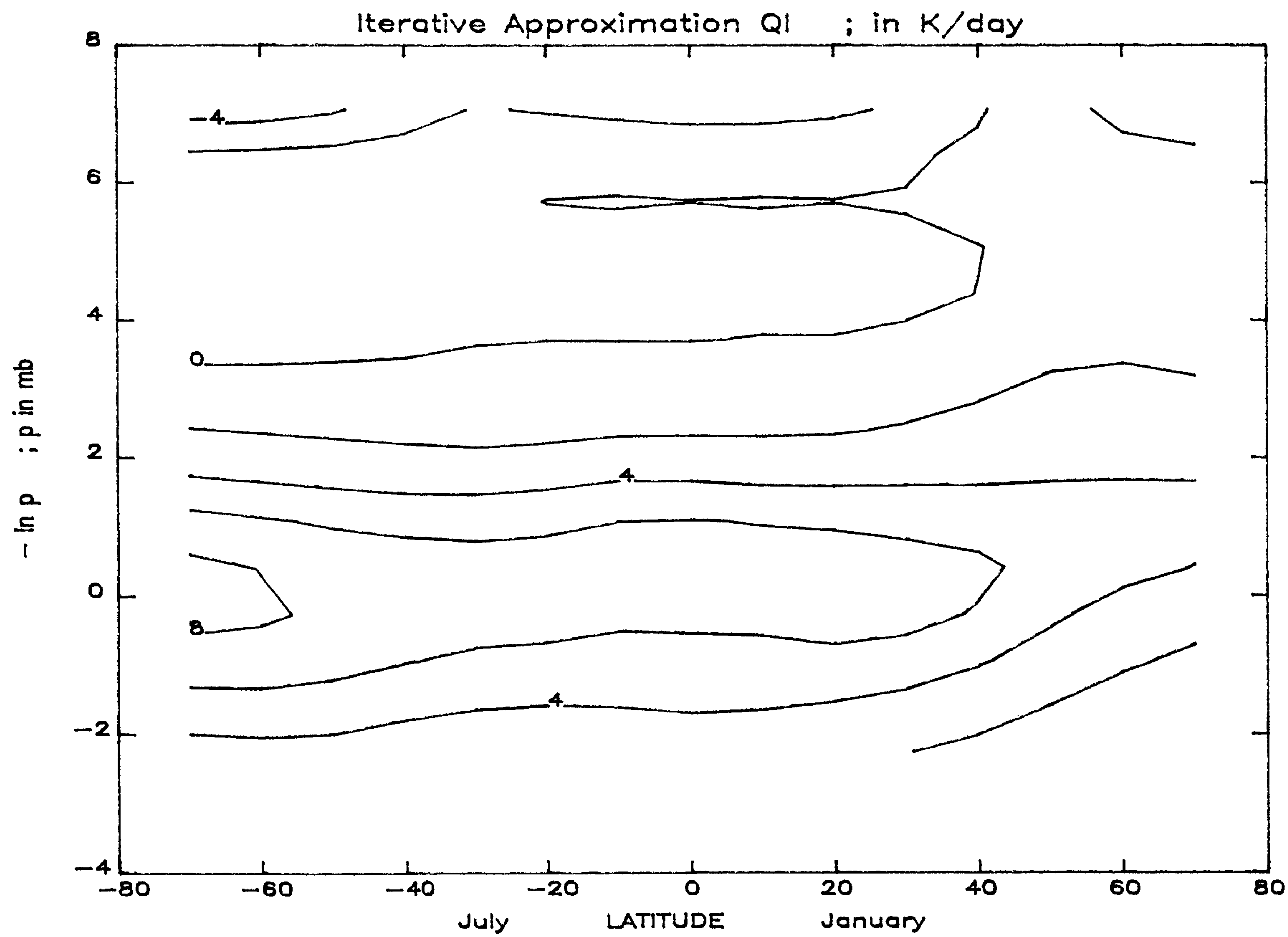

Iterative Approximation QI ; in K/day
8
6
4
2
0
−2
−4
−80
−60
−40
−20
0
20
40
60
80
July
LATITUDE
January
− ln p ; p in mb
−4
0
4
8
4

Figure 9

0.96574651	-3.42534885E-02	-3.42534885E-02	-3.42534885E-02	-3.42534885E-02	-3.42534885E-02	-3.42534885E-02	-3.42534885E-02
-3.42534885E-02	-3.42534885E-02	-3.42534885E-02	-3.42534885E-02	-3.42534885E-02	-3.42534885E-02	-3.42534885E-02	
-2.93437783E-02	0.97065622	-2.93437783E-02	-2.93437783E-02	-2.93437783E-02	-2.93437783E-02	-2.93437783E-02	-2.93437783E-02
-2.93437783E-02	-2.93437783E-02	-2.93437783E-02	-2.93437783E-02	-2.93437783E-02	-2.93437783E-02	-2.93437783E-02	
-2.68601848E-02	-2.68601848E-02	0.97313982	-2.68601848E-02	-2.68601848E-02	-2.68601848E-02	-2.68601848E-02	-2.68601848E-02
-2.68601848E-02	-2.68601848E-02	-2.68601848E-02	-2.68601848E-02	-2.68601848E-02	-2.68601848E-02	-2.68601848E-02	
-2.81069718E-02	-2.81069718E-02	-2.81069718E-02	0.97189303	-2.81069718E-02	-2.81069718E-02	-2.81069718E-02	-2.81069718E-02
-2.81069718E-02	-2.81069718E-02	-2.81069718E-02	-2.81069718E-02	-2.81069718E-02	-2.81069718E-02	-2.81069718E-02	
-2.79403969E-02	-2.79403969E-02	-2.79403969E-02	-2.79403969E-02	0.97205960	-2.79403969E-02	-2.79403969E-02	-2.79403969E-02
-2.79403969E-02	-2.79403969E-02	-2.79403969E-02	-2.79403969E-02	-2.79403969E-02	-2.79403969E-02	-2.79403969E-02	
-2.92073421E-02	-2.92073421E-02	-2.92073421E-02	-2.92073421E-02	-2.92073421E-02	0.97079266	-2.92073421E-02	-2.92073421E-02
-2.92073421E-02	-2.92073421E-02	-2.92073421E-02	-2.92073421E-02	-2.92073421E-02	-2.92073421E-02	-2.92073421E-02	
-3.27919547E-02	-3.27919547E-02	-3.27919547E-02	-3.27919547E-02	-3.27919547E-02	-3.27919547E-02	0.96720805	-3.27919547E-02
-3.27919547E-02	-3.27919547E-02	-3.27919547E-02	-3.27919547E-02	-3.27919547E-02	-3.27919547E-02	-3.27919547E-02	
-3.04373010E-02	-3.04373010E-02	-3.04373010E-02	-3.04373010E-02	-3.04373010E-02	-3.04373010E-02	-3.04373010E-02	0.96956270
-3.04373010E-02	-3.04373010E-02	-3.04373010E-02	-3.04373010E-02	-3.04373010E-02	-3.04373010E-02	-3.04373010E-02	
-3.17769666E-02	-3.17769666E-02	-3.17769666E-02	-3.17769666E-02	-3.17769666E-02	-3.17769666E-02	-3.17769666E-02	-3.17769666E-02
0.96822303	-3.17769666E-02	-3.17769666E-02	-3.17769666E-02	-3.17769666E-02	-3.17769666E-02	-3.17769666E-02	
-3.31959363E-02	-3.31959363E-02	-3.31959363E-02	-3.31959363E-02	-3.31959363E-02	-3.31959363E-02	-3.31959363E-02	-3.31959363E-02
-3.31959363E-02	0.96680406	-3.31959363E-02	-3.31959363E-02	-3.31959363E-02	-3.31959363E-02	-3.31959363E-02	
-3.66545704E-02	-3.66545704E-02	-3.66545704E-02	-3.66545704E-02	-3.66545704E-02	-3.66545704E-02	-3.66545704E-02	-3.66545704E-02
-3.66545704E-02	-3.66545704E-02	0.96334543	-3.66545704E-02	-3.66545704E-02	-3.66545704E-02	-3.66545704E-02	
-3.34892605E-02	-3.34892605E-02	-3.34892605E-02	-3.34892605E-02	-3.34892605E-02	-3.34892605E-02	-3.34892605E-02	-3.34892605E-02
-3.34892605E-02	-3.34892605E-02	-3.34892605E-02	0.96651074	-3.34892605E-02	-3.34892605E-02	-3.34892605E-02	
-2.43428294E-02	-2.43428294E-02	-2.43428294E-02	-2.43428294E-02	-2.43428294E-02	-2.43428294E-02	-2.43428294E-02	-2.43428294E-02
-2.43428294E-02	-2.43428294E-02	-2.43428294E-02	-2.43428294E-02	0.97565717	-2.43428294E-02	-2.43428294E-02	
-2.70849169E-02	-2.70849169E-02	-2.70849169E-02	-2.70849169E-02	-2.70849169E-02	-2.70849169E-02	-2.70849169E-02	-2.70849169E-02
-2.70849169E-02	-2.70849169E-02	-2.70849169E-02	-2.70849169E-02	-2.70849169E-02	0.97291508	-2.70849169E-02	
-3.54123574E-02	-3.54123574E-02	-3.54123574E-02	-3.54123574E-02	-3.54123574E-02	-3.54123574E-02	-3.54123574E-02	-3.54123574E-02
-3.54123574E-02	-3.54123574E-02	-3.54123574E-02	-3.54123574E-02	-3.54123574E-02	-3.54123574E-02	0.96458764	

Table 1

ORIGINAL PAGE IS
OF POOR QUALITY

```
OPENR,1,'TEST'
OPENR,2,'TESQ'
OPENR,3,'MLP'
OPENR,4,'TESI'
OPENR,5,'C'
T = DBLARR(15,15) ; in K
Q = DBLARR(15,15) ; in K/day
MLP = DBLARR(15)
I = DBLARR(15,15)
C = DBLARR(15,15)
READF,1,T
READF,2,Q
READF,3,MLP
READF,4,I
READF,5,C
CLOSE,1
CLOSE,2
CLOSE,3
CLOSE,4
CLOSE,5
KB = 1.38062E-16 ; erg/K
RC = 3.3E-4 ; mixing ratio of CO2
NL = 2.69E19 ; loschmidt's number, in cm^-3
S = 242*SQRT(T/273)
X = 960.0/T
B = 97.1*S/(EXP(X)-1)
P = DBLARR(15,15)
FOR L = 0,14 DO P(*,L)=EXP(-MLP(L)) ; P in mb
N = RC * P * 1000 /(KB * T) ; in #/cm^3, the 1000 is mb to dyne/cm^2
;                to check n, @ 85 km n(CO2)=10^11/cm^3
PHI = 24 * P / 1.013 ; dimensionless
E = 1/(4 * 3.1416 * S * N * PHI)
K1 = 4.11E11
K2 = 81.12
J = B/K2 + K1*E*Q
QT = J # C
XY = FINDGEN(15)
L = (XY - 7)*10
A = MLP
; Try iterative technique
JI = B/K2
     FOR K = 0,4 DO BEGIN
     QI = JI # C
     JI = B/K2 + K1*E*QI
     END
QI = JI # C
END
```